

# Enhancement and Stability of Reactive Oxygen and Nitrogen Species in Water Treatment Processes Using Cold Plasma

Suvarna Patil<sup>1\*</sup>, Umesh Chavan<sup>1</sup>

<sup>1</sup> Vishwakarma Institute of Technology, Pune 411037, Maharashtra, India

\* Corresponding author, e-mail: [suvarna.mane@vit.edu](mailto:suvarna.mane@vit.edu)

Received: 21 August 2025, Accepted: 04 February 2026, Published online: 11 March 2026

## Abstract

Cold plasma technology has significant potential for application in water treatment due to its capacity to generate highly reactive oxygen and nitrogen species (RONS). This study compared the performance of dielectric barrier discharge (DBD) and corona discharge (CD) plasma reactors, both operated using ambient air, to evaluate the influence of reactor geometry on RONS generation under identical operating conditions. Comparative analysis showed that the CD method consistently produced higher concentrations of RONS, including  $\text{H}_2\text{O}_2$ ,  $\text{NO}_2^-$ ,  $\text{NO}_3^-$ , and  $\text{O}_3^-$ , than the DBD system. Based on this superior performance, the CD method was selected for a detailed investigation into the effects of treatment time and water volume, and, crucially, the temporal stability of RONS. The long-term analysis revealed that hydrogen peroxide ( $\text{H}_2\text{O}_2$ ) and nitrate ( $\text{NO}_3^-$ ) are relatively stable in plasma-activated water (PAW) over a week of storage, while ozone ( $\text{O}_3$ ) and nitrite ( $\text{NO}_2^-$ ) were unstable, with  $\text{O}_3$  rapidly decomposing and  $\text{NO}_2^-$  converting into the stable  $\text{NO}_3^-$ . This PAW, rich in stable RONS, demonstrated strong microbicidal activity, achieving over 90% inactivation against single and mixed bacterial cultures (including *E. coli*, *P. aeruginosa*, and *S. aureus*). These findings not only identify the CD configuration as the more efficient plasma generation method but also provide critical insights into RONS transformation pathways and the storage potential of PAW, highlighting its viability as a sustainable approach for water quality enhancement.

## Keywords

dielectric barrier discharge, corona discharge, plasma reactor, reactive oxygen and nitrogen species, plasma-activated water

## 1 Introduction

Water scarcity continues to intensify worldwide due to the rapid depletion and contamination of freshwater resources. Industrial expansion, population growth, and the emergence of persistent organic pollutants have exposed the limitations of conventional water treatment technologies, emphasizing the need for sustainable and scalable alternatives [1]. Cold plasma, a non-thermal ionized gas containing electrons, ions, and neutral species, has emerged as a promising tool for water purification owing to its ability to operate under ambient conditions and generate a diverse mixture of reactive oxygen and nitrogen species (RONS) in aqueous systems [2]. During plasma–liquid interaction, species such as hydrogen peroxide ( $\text{H}_2\text{O}_2$ ), ozone ( $\text{O}_3$ ), nitrite ( $\text{NO}_2^-$ ), and nitrate ( $\text{NO}_3^-$ ) are produced, offering strong oxidative capability for microbial inactivation, pollutant degradation, and advanced oxidation processes [3]. Dielectric barrier discharge (DBD) [4] and corona discharge (CD) [5] are two widely used atmospheric-pressure

plasma configurations, yet direct comparisons of their RONS-generation behaviour under identical operating conditions remain scarce. Previous study [6], focused primarily on reactor innovation and performance enhancement, introducing a novel multi-compartment dielectric barrier discharge (MCDBD) design aimed at scaling up the treatment process to activate larger volumes of water efficiently. Research advancements, including microbubble-enhanced plasma systems and pulsed-DBD configurations, have shown improved mass transfer, higher inactivation efficiencies, and strong dependence on water matrix composition, highlighting the complex chemistry governing plasma-activated water (PAW) [7, 8]. Various international standards are available for the measurement of reactive species in aqueous systems, ensuring accuracy and reliability in quantifying plasma-generated species [9–11]. Among these, understanding the formation pathways [12, 13] of  $\text{H}_2\text{O}_2$  is particularly important, as it often acts as a precursor that

influences the generation and stability of other reactive oxygen and nitrogen species crucial for disinfection [14, 15]. Ozone, another major species produced during plasma–liquid shapes the overall composition of reactive nitrogen species in plasma-activated water [16, 17]. A comprehensive understanding of these species, along with accurate measurement techniques, is therefore essential for optimizing the performance and application of plasma-activated water. The novelty of this study lies in its direct comparison of CD and DBD plasma systems, both operated under the same air atmosphere, voltage, and treatment time. The corona discharge produces unrestricted micro discharges that interact directly with the water surface, while the dielectric barrier in the DBD setup restricts current flow and disperses the discharge, altering how reactive species are transferred into the liquid. By tracking the behaviour of  $\text{H}_2\text{O}_2$ ,  $\text{O}_3$ ,  $\text{NO}_2^-$ , and  $\text{NO}_3^-$  over time, the work uncovers how these reactive oxygen and nitrogen species are connected through a chain of oxidation and reduction reactions. The rise or depletion of one species influences the next, creating a dynamic chemical balance within plasma-activated water. This mechanistic insight into how discharge geometry shapes both RONS formation and persistence offers a clearer path to designing efficient plasma systems for water treatment. The current paper emphasizes comparative study and temporal analysis. Two distinct reactor configurations: DBD and CD are considered under consistent operating conditions to determine which is superior at generating RONS. This research goes beyond mere generation to thoroughly investigate the long-term stability (lifetime) of these reactive species within the plasma-activated water. Providing essential data for practical application and storage, which was not the core objective of the previous study, which was design-focused [6].

## 2 Methodology

### 2.1 Dielectric barrier discharge plasma setup

The DBD system employed a pin-to-plate configuration to generate non-thermal plasma at atmospheric pressure. A quartz plate (1 mm thickness) was used as the dielectric barrier owing to its excellent thermal stability and insulation properties. The plate was fixed at the base of a cylindrical container containing the treatment water. The bottom electrode, made of stainless steel (SS 304), was attached beneath the quartz plate, whereas the top electrode, also made of SS 304 in a pin-type geometry, was positioned 3 mm above the water surface. Plasma was initiated using a high-voltage AC power supply delivering 3 kV peak-to-peak at 20 kHz with a discharge current of 30 mA.

The working gas was ambient air, and no external gas flow was introduced. A plasma–liquid interaction occurred in the air gap between the top electrode and the water surface. To evaluate the influence of treatment parameters, experiments were conducted for a water volume of 200 mL for 15 min of treatment time. All the experiments were performed at room temperature and atmospheric pressure. A schematic of the DBD setup is shown in Fig. 1(a).

### 2.2 Corona discharge plasma setup

The CD plasma system utilized a pin-to-pin electrode configuration designed to enhance the direct plasma–liquid interaction. Both electrodes were fabricated from stainless steel (SS 304). One electrode was immersed in the water sample, while the other was positioned 3 mm above the water surface, aligned vertically to maintain the same electrode tip-to-water-surface gap as in the DBD system.

The same high-voltage AC power supply (3 kV peak-to-peak, 20 kHz, 30 mA) was used to generate the corona discharge. Ambient air served as the discharge medium with no additional gas input, ensuring parity with the

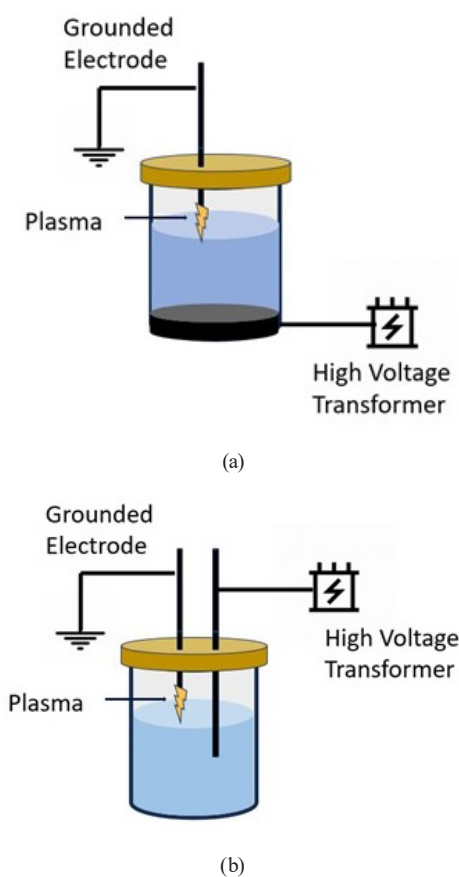


**Fig. 1** Scheme of different methods for PAW generation: (a) dielectric barrier discharge method, (b) corona discharge method

DBD experiments. The immersed electrode acted as a discharge target, promoting efficient species transfer into the water. A water volume of 200 mL was treated for 15 min. All discharges were generated at room temperature and at atmospheric pressure.

Table 1 shows the parameters used during the experiments. The CD configuration allowed for a direct comparison with the DBD setup by eliminating the dielectric barrier and altering the electrode–water interface geometry. A schematic representation of the CD system is shown in Fig. 1(b). After comparison of the two methods based on results, the CD method was applied for the analysis of various reactive species. To understand the time-based evaluation of species, 200, 300 and 400 mL of water (15 mm, 22.5 mm and 30 mm thickness) were treated for different durations (10 min, 20 min, 30 min, 40 min, 50 min, 60 min). Readings were taken immediately after treatment.

To understand the stability of reactive species 200 mL of water was treated for different time duration ranging from 10 to 60 min with steps of 10 min. Stored in different containers and reading were taken for 1 week for every 24 h.

### 2.3 Measurement of reactive species

RONS generated in the plasma-treated water were quantified using Aquasol water testing kits, which adhere to standard protocols based on the APHA/AWWA/IS guidelines [9–11]. The measurement methods and corresponding chemical reactions for each species are described below.

#### 2.3.1 H<sub>2</sub>O<sub>2</sub> measurement

The concentration of hydrogen peroxide in PAW was measured using the AQUASOL AEHP - Hydrogen Peroxide Test Kit, which is based on a color-disappearance titrimetric method. A 10 mL sample was transferred into the test vial, followed by the addition of 20 drops of reagent HP-1

and thorough mixing. Then, two spoonfuls of reagent HP-2 were added to initiate the color reaction. Reagent HP-3 was added dropwise until the solution turned completely colorless, indicating the endpoint.

The hydrogen peroxide concentration was calculated directly using the manufacturer-provided calibration chart based on the number of HP-3 drops used. This validated method is widely applied in water-treatment and disinfectant monitoring and is suitable for oxidant-rich matrices such as plasma-activated water.

#### 2.3.2 Nitrite and nitrate measurement

##### *Nitrite measurement*

Nitrite concentration was measured using the AQUASOL AE207 – nitrite test kit which operates on the standard colorimetric diazotization–coupling reaction (Griess method). In this procedure, nitrite (NO<sub>2</sub><sup>-</sup>) present in the sample reacts with sulfanilic acid under acidic conditions to form a diazonium salt. This intermediate subsequently couples with N-(1-naphthyl)ethylenediamine dihydrochloride (NED), producing a characteristic pink-to-red azo dye. The intensity of the developed color is directly proportional to the nitrite concentration. After adding the kit reagents, the sample color is compared visually with the standardized color chart provided by the manufacturer, allowing semi-quantitative estimation of nitrite levels (mg/L).

##### *Nitrate measurement*

Nitrate concentration was measured using the AQUASOL AE308 – nitrate test kit, in which nitrate is reduced to nitrite using the kit's reducing reagent, followed by titrimetric color-based quantification using the same color comparison principle.

#### 2.3.3 O<sub>3</sub> measurement

Ozone concentration was measured using the AQUASOL AEOZ3H – Ozone Test Kit. In this titrimetric iodometric method, ozone oxidizes iodide ions in a phosphate-buffered solution, producing iodine that forms a pink-colored complex with N,N-diethyl-p-phenylenediamine (DPD). The pink color is titrated with sodium thiosulfate until complete disappearance, with the amount of thiosulfate consumed directly proportional to the ozone concentration.

All analytical procedures were performed in accordance with standard protocols (e.g., Method 4500-C1 F) described in "Standard Methods for the Examination of Water and Wastewater" [11] published by APHA. All measurements were performed in triplicate, and the average

**Table 1** Operating parameters for different plasma generators

| Parameter             | Value                                  |
|-----------------------|--|
| Electrode material    | Stainless steel (SS 304)               |
| Electrode gap         | 3 mm                                   |
| Input voltage         | 3 kV (peak-to-peak)                    |
| Current               | 30 mA                                  |
| Working gas           | Ambient air (no external flow)         |
| Water volumes treated | 200 mL                                 |
| Water thickness       | 10 mm                                  |
| Treatment durations   | 15 min                                 |
| Operating conditions  | Atmospheric pressure, room temperature |

values were used for analysis. Proper calibration and blank correction were performed according to the kit instructions. All measurements were conducted immediately after plasma activation to avoid the decay of the species.

### 2.3.4 Microbial inactivation testing

For the microbial inactivation study, *Escherichia coli* (1 mL containing  $1 \times 10^8$  CFU) was added to 200 mL of tap water and plasma-activated water (PAW) generated using the corona discharge method. After 5 min of exposure, CFU counts were determined to evaluate the bactericidal efficiency of PAW.

For the mixed-culture inactivation study, a suspension containing *E. coli*, *Pseudomonas aeruginosa* and *Staphylococcus aureus* (1 mL with  $1 \times 10^8$  CFU) was added to 200 mL of tap water and PAW. After 10 min of exposure the CFU counts were measured to assess the inactivation efficiency.

## 3 Results and discussion

Table 2 shows a comparative analysis of the water quality parameters, revealing significant variations between untreated water and water subjected to DBD and CD plasma treatments. The pH of water was slightly increased after plasma treatment. Both discharge systems generated hydrogen peroxide, nitrite, nitrate, and ozone, with the corona discharge consistently producing higher concentrations than the dielectric barrier discharge. 200 mL of water was treated with corona discharge and dielectric barrier discharge method for 15 min (thickness 15 mm).

The results indicate that both plasma treatment methods effectively modified the physicochemical properties of water; however, CD consistently produced higher levels of reactive oxygen and nitrogen species than DBD. Initially, the pH increases slightly but is subsequently reduced. The greater decrease in pH after CD treatment suggests a higher dissolution of acidic oxides, primarily nitric and nitrous acids, formed through plasma-induced reactions.

**Table 2** Water quality parameters before and after DBD and CD treatments

| Parameter                     | Value | Before treatment | After DBD treatment | After CD treatment |
|-------------------------------|-------|------------------|---------------------|--------------------|
| H <sub>2</sub> O <sub>2</sub> | mg/L  | 0                | 15                  | 20                 |
| NO <sub>2</sub> <sup>-</sup>  | mg/L  | 0                | 7                   | 15                 |
| NO <sub>3</sub> <sup>-</sup>  | mg/L  | 0                | 7                   | 20                 |
| O <sub>3</sub>                | mg/L  | 0                | 1.5                 | 3                  |
| pH                            | –     | 6.5              | 7.0                 | 7.0                |
| EC*                           | μS/cm | 680              | 726                 | 928                |

\*Electrical conductivity

The higher concentrations of nitrite and nitrate observed in CD-treated water arise from the stronger local electric fields generated at the corona electrode tip, which produce a larger population of energetic electrons at the air–water interface. These electrons efficiently dissociate N<sub>2</sub> and O<sub>2</sub>, thereby enhancing the formation of reactive nitrogen species that subsequently dissolve and convert into nitrite and nitrate in the liquid phase. In contrast, the dielectric barrier in the DBD configuration restricts current flow and distributes the plasma over a wider region, which reduces both the peak electron density and the mean electron energy. As a result, electron-impact reactions leading to reactive nitrogen species (RNS) formation occur less intensively in DBD, whereas the direct, barrier-free corona discharge sustains a more localized, dense electron environment that favours higher RNS production. Elevated hydrogen peroxide and ozone concentrations in CD-treated water confirmed its higher oxidative potential, likely linked to a greater electron density and higher generation rates of hydroxyl and atomic oxygen radicals. Overall, the comparative analysis demonstrated that CD treatment is more effective than DBD in generating oxidative and nitrogenous reactive species, which may enhance its applicability in advanced water treatment processes. Based on the analysis the CD method was used for further time based and stability analysis of RONS.

### 3.1 Hydrogen peroxide

In the gas phase, hydroxyl radicals ( $\cdot\text{OH}$ ) are primarily generated through oxygen-atom interactions and electron-impact dissociation of water vapor. In the liquid phase, the dominant route for H<sub>2</sub>O<sub>2</sub> formation is the recombination of dissolved  $\cdot\text{OH}$  radicals [12, 13].



Water was treated for 10 to 60 min with step of 10 min for volume of 200, 300 and 400 mL. The results (Fig. 2) show that the H<sub>2</sub>O<sub>2</sub> concentration increased consistently over time for 200 mL of water. In contrast, for 300 mL and 400 mL of water, the concentration initially increased but then decreased, which can be attributed to the decomposition of H<sub>2</sub>O<sub>2</sub> into H<sub>2</sub>O over time. The decomposition pathway involves reactions with hydroxyl radicals (Eqs. (4) and (5)), producing hydroperoxyl radicals ( $\cdot\text{HO}_2$ )

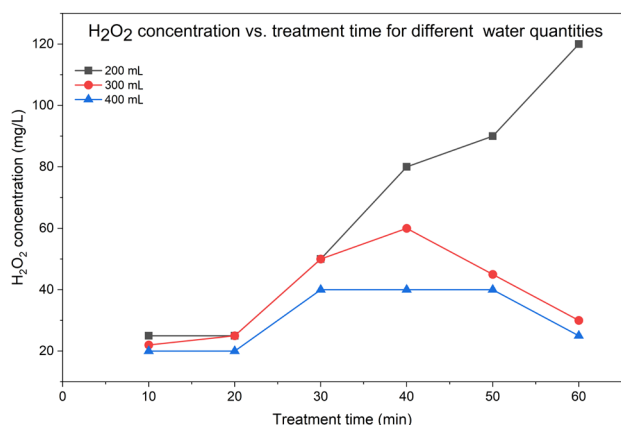


**Fig. 2** Effect of treatment time on H<sub>2</sub>O<sub>2</sub> concentration at different water volumes

and ultimately oxygen and water.



The highly reactive hydroxyl radical ( $\cdot\text{OH}$ ) readily decomposes hydrogen peroxide into the more stable hydroperoxyl radical ( $\cdot\text{HO}_2$ ), which then reacts with another  $\cdot\text{OH}$  radical to produce oxygen and water. This explains the decreasing trend in H<sub>2</sub>O<sub>2</sub> concentration for larger water volumes, where the decomposition rate exceeded the generation rate [14, 15]. But with a smaller water volume, the same discharge power produces a higher density of plasma-generated radicals ( $\cdot\text{OH}$ ). Their rapid recombination forms H<sub>2</sub>O<sub>2</sub> faster than it can decompose, leading to net accumulation.

To further investigate H<sub>2</sub>O<sub>2</sub> stability in PAW, measurements were taken daily for up to one week. Fig. 3 shows that the H<sub>2</sub>O<sub>2</sub> concentration decreased slowly during the first four days, after which it stabilised and remained

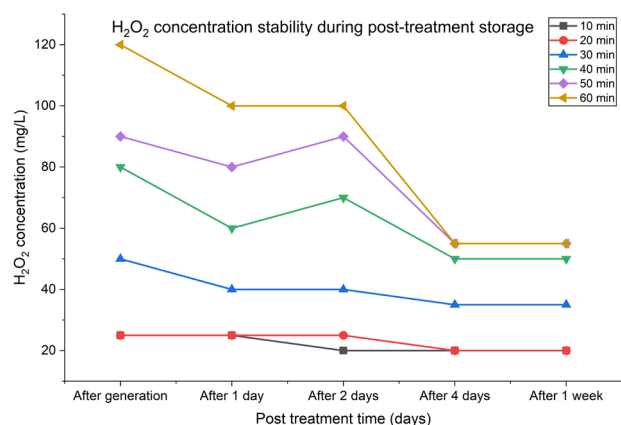


**Fig. 3** Long-term stability of H<sub>2</sub>O<sub>2</sub> in plasma-activated water over one week for 200 mL at different treatment times

constant for a longer period. This indicates that H<sub>2</sub>O<sub>2</sub> in PAW is relatively stable, allowing it to be stored for later use in applications that require oxidative potential.

### 3.2 Ozone

Another important oxygen-based reactive species in plasma-activated water is ozone. Its concentration in water is relatively low because of the complexity of ozone dissolution and its rapid reaction with atomic oxygen (O) to form more stable molecular oxygen (O<sub>2</sub>) [18]. Nevertheless, trace amounts of ozone were detected shortly after plasma treatment. Fig. 4 illustrates the variation in the ozone concentration over time for different water volumes.

Ozone formation begins with the dissociation of molecular oxygen into atomic oxygen via electron impact (Eq. (6)). Atomic oxygen then reacts with molecular oxygen in the presence of a third body (M) to form ozone (Eq. (7)) [19].



However, ozone is unstable in aqueous environment. It decomposes when atomic oxygen interacts with ozone, producing molecular oxygen (Eq. (8)) [20].



As shown in Fig. 4, ozone generation is unstable owing to its high reactivity with atomic oxygen, leading to a rapid decline in concentration after plasma treatment. Fig. 5 further demonstrates the ozone stability over time, where the species becomes undetectable after a few days. This instability is attributed to its transformation into molecular oxygen, which is thermodynamically more stable under aqueous conditions.

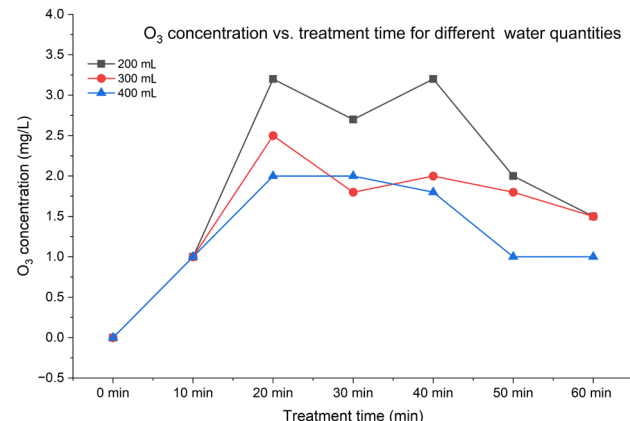


**Fig. 4** Effect of treatment time on O<sub>3</sub> concentration at different water volumes

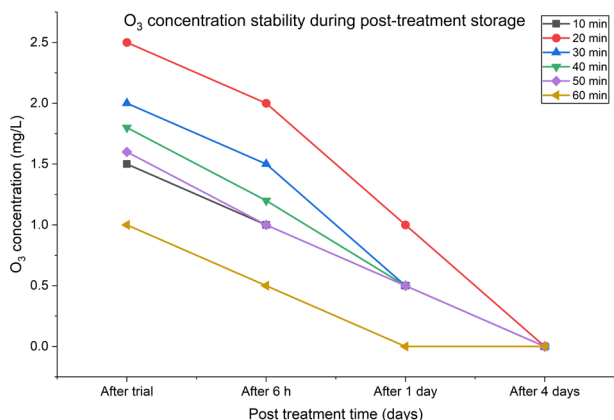


Fig. 5 Long-term stability of O<sub>3</sub> in plasma-activated water over one week for 200 mL at different treatment times

### 3.3 Nitrite

The formation of nitric oxide ( $\cdot\text{NO}$ ) plays a crucial role in generating RNS in PAW [21, 22]. Nitrite ( $\text{NO}_2^-$ ) is a relatively stable species present in PAW. The interaction of nitric oxide with atomic oxygen (O) leads to the formation of nitrogen dioxide ( $\cdot\text{NO}_2$ ), as shown in reaction (Eq. (9)), which is an important pathway for nitrite production:



Additionally, nitric oxide reacts with ozone, formed during plasma treatment, to yield nitrogen dioxide and molecular oxygen, which are more stable products than ozone (Eq. (10)) [23, 24]:



Another significant route for nitrite formation is the reaction of nitric oxide with the hydroperoxyl radical ( $\cdot\text{HO}_2$ ), generated during the decomposition of hydrogen peroxide, producing nitrogen dioxide and hydroxyl radicals reaction (Eq. (11)) [25].



Furthermore, when electronically excited nitric oxide ( $\cdot\text{NO}^*$ ) transfers its energy to molecular oxygen, it produces nitrogen dioxide and atomic oxygen reaction (Eq. (12)) [26].



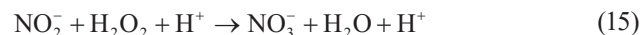
Hydration of  $\cdot\text{NO}_2$  Takes place once it enters into water (Eq. (13)) [27].



Nitrous acid is weak acid as it forms immediately converts it into nitrite in liquid phase (Eq. (14)).



Fig. 6 shows nitrite concentration with reference to treatment time. The trend shows that it increases along with the treatment time, but is affected due to oxidation of nitrite to nitrate in the presence of hydrogen peroxide (Eq. (15)).



To better understand the conversion of nitrite to nitrate, the evolution of pH with treatment time was also monitored (Fig. 7). The results show a gradual decrease in pH as the treatment time increases, indicating progressive acidification of the plasma-activated water due to the dissolution of nitrogen oxides and the formation of nitrous and nitric acids. Under these mildly acidic conditions, reaction Eq. (15) becomes more favourable, promoting the oxidation of nitrite to nitrate in the presence of hydrogen peroxide. This behaviour explains the simultaneous

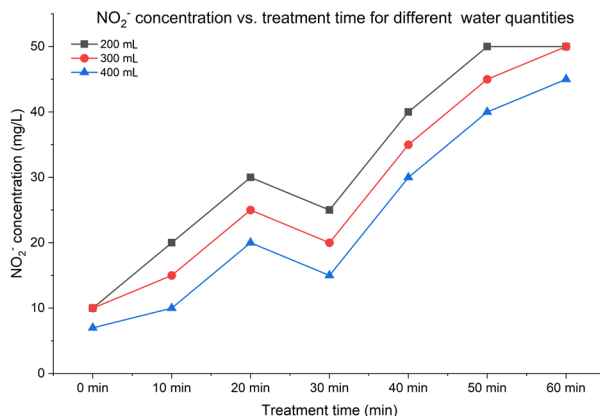


Fig. 6 Effect of treatment time on Nitrite concentration at different water volumes

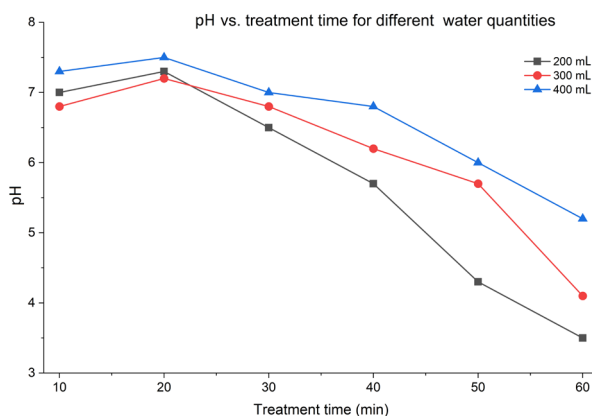


Fig. 7 Effect of treatment time on pH evaluation at different water volumes

decrease in nitrite and increase in nitrate observed at longer treatment times, confirming the mechanistic role of Eq. (15) in the nitrogen species transformation pathway.

### 3.4 Nitrate

When nitrite is oxidised to nitrate in the presence of hydrogen peroxide, as shown in reaction Eq. (13), nitrite acts as an intermediate species. Therefore, the concentration of nitrate in PAW is directly influenced by the amount of nitrite present in the water [18, 28, 29].

Fig. 8 shows the variation in nitrate concentration with different treatment times. The trend closely follows the crease in nitrite concentration observed in the previous figure, indicating that nitrate formation is linked to the availability of nitrite.

Fig. 9 presents the stability of nitrate in PAW over a post-treatment period of up to one week. The results reveal that nitrate remains stable during storage. A slight increase in nitrate concentration is observed in the initial days, which can be attributed to the continued oxidation of nitrite into nitrate in the presence of hydrogen

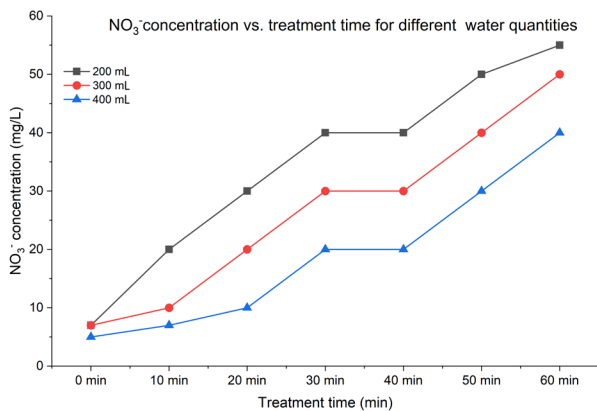


Fig. 8 Effect of treatment time on nitrate concentration at different water volumes

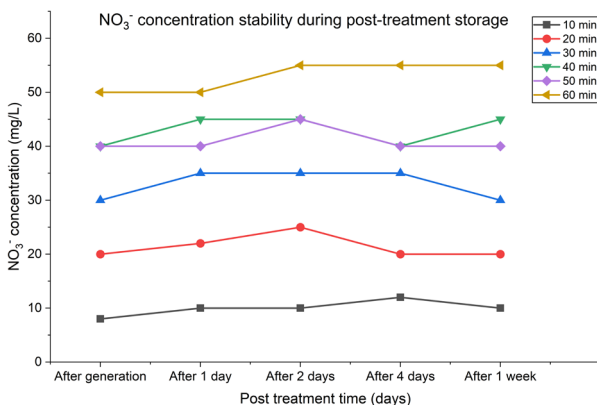


Fig. 9 Long-term stability of nitrate in plasma-activated water over one week for 200 mL at different treatment times

peroxide (Eq. (15)). Over time, the nitrite concentration becomes negligible as it is completely converted to nitrate. Consequently, hydrogen peroxide concentration also stabilises after this conversion is complete [16, 17].

### 3.5 Microbial decontamination

The testing procedure was designed to evaluate the inactivation efficacy of PAW against both single and mixed bacterial cultures by following standard protocols based on the APHA/AWWA/IS guidelines [9–11]. Results are compared from the CD and DBD treatments. PAW was generated using both the CD and DBD plasma reactors. The plasma activated water produced by treating 200 mL of tap water. Single-culture (*Escherichia coli*) and mixed-culture (*E. coli* and *S. aureus*) inactivation test are performed. The test method is the most common and robust way to quantify disinfection efficacy. Quantitative surface carrier test procedure is followed as below.

- Inoculation (Control): Prepared a high-concentration bacterial suspension (e.g., 10<sup>8</sup> CFU/mL) of the *E. coli*, *S. aureus*.
- Target surface preparation: Selected a standardized, non-porous surface material stainless steel and glass that represents the target application surface.
- PAW treatment: Applied the 1 mL of PAW to the targeted dried surface by wiping with a PAW saturated cloth.
- Treatment time: Controlled the contact time 5 min and temperature.
- Efficacy calculation: The results are reported as log reduction (LR), which is the standard industry measure for disinfectant performance:  $LR = \log_{10}(\text{CFU Control}) - \log_{10}(\text{CFU Treated})$

Figs. 10 and 11 show the comparative inactivation effects of PAW generated by corona and dielectric barrier discharges (DBD) against single and mixed bacterial cultures.

The results demonstrated a significant reduction in bacterial colony-forming units (CFU) in both corona discharge



Fig. 10 Microbiocidal inactivation testing - bacteria *E. coli* treatment time 5 min. (a) Tap water, (b) plasma activated water (corona discharge), (c) plasma activated water (dielectric barrier discharge)



**Fig. 11** Microbiocidal inactivation testing - bacteria mix culture of *E. coli*, *Pseudomonas aeruginosa* and *Staphylococcus aureus*, treatment time

and DBD-treated PAW compared to tap water. In both single and mixed culture experiments, more than 90% bacterial inactivation was achieved with the PAW. This strong bactericidal activity can be attributed to the synergistic effects of reactive oxygen species and RNS in PAW, which damage bacterial cell membranes, disrupt intracellular components, and ultimately lead to cell death.

These findings confirm that the high oxidative potential of PAW renders it an effective antimicrobial agent, highlighting its potential application in water and wastewater treatment processes.

#### 4 Conclusion

Plasma-activated water was generated using two plasma generators: corona discharge and dielectric barrier

discharge. Among these, the corona discharge method is relatively simple and generates reactive species more effectively. The generation of hydrogen peroxide is primarily driven by the formation of hydroxyl radicals and increases over time. However, its concentration is influenced by the reduction of nitrite to nitrate.  $H_2O_2$  also exhibits good stability, remaining effective for a longer duration. Ozone is an unstable reactive species owing to its high reactivity with atomic oxygen, forming molecular oxygen, which is more stable. Consequently, ozone was not traceable after the post-treatment period. Nitrite is an intermediate species in nitrate formation. During treatment, its concentration increases over time but becomes undetectable after post-treatment because it is converted into nitrate. In contrast, nitrate remained stable in the PAW for an extended period. Since PAW contains hydrogen peroxide and ozone, it exhibits strong disinfectant properties, making it effective for the deactivation of various microbes. Considering the properties of PAW and the stability of reactive species, it can be widely used in applications such as water purification, medical disinfection and agriculture. However, further studies are required to explore its large-scale implementation and environmental safety issues.

#### References

- [1] Sahoo, P. K., Sarkar, D., Rahman, M. M., Datta, R. "Sustainable Environmental Technologies: Recent Development, Opportunities, and Key Challenges", *Applied Sciences*, 14(23), 10956, 2024. <https://doi.org/10.3390/app142310956>
- [2] El Shaer, M., Eldaly, M., Heikal, G., Sharaf, Y., Diab, H., Mobasher, M., Rousseau, A. "Antibiotics Degradation and Bacteria Inactivation in Water by Cold Atmospheric Plasma Discharges Above and Below Water Surface", *Plasma Chemistry and Plasma Processing*, 40(4), pp. 971–983, 2020. <https://doi.org/10.1007/s11090-020-10076-0>
- [3] Dharini, M., Jaspin, S., Mahendran, R. "Cold plasma reactive species: Generation, properties, and interaction with food biomolecules", *Food Chemistry*, 405, 134746, 2022. <https://doi.org/10.1016/j.foodchem.2022.134746>
- [4] Ghernaout, D., Elboughdiri, N. "Disinfecting Water: Plasma Discharge for Removing Coronaviruses", *Open Access Library Journal*, 7(4), e6314, 2020. <https://doi.org/10.4236/oalib.1106314>
- [5] Gururani, P., Bisht, B., Kumar, V., Joshi, N. C., Tomar, M. S., Pathak, B. "Cold plasma technology: advanced and sustainable approach for wastewater treatment", *Environmental Science and Pollution Research*, 28(46), pp. 65062–65082, 2021. <https://doi.org/10.1007/s11356-021-16741-x>
- [6] Chavan, U., Hulwan, D., Harad, A., Gham, A., Bagale, P., Aphale, S., Ajgaonkar, S. "Development of Multi-Compartment Dielectric Barrier Discharge Plasma Reactor for Innovative Water Treatment", *Periodica Polytechnica Chemical Engineering*, 68(4), pp. 531–540, 2024. <https://doi.org/10.3311/ppch.36688>
- [7] Kuddushi, M., Dal, P., Xiaoyun, C., Xincong, Q., Luo, J., Gan, H., Lu, D., Zhu, D. Z. "Microbubble-Enhanced Cold Plasma (MB-CAP) for Pathogen Disinfection in Water: A Sustainable Alternative to Traditional Methods", *Materials Horizons*, 12(21), pp. 8774–8801, 2025. <https://doi.org/10.1039/d5mh00945f>
- [8] Triantaphyllidou, I.-E., Aggelopoulos, C. A. "Insights on Bacteria Inactivation in Water by Cold Plasma: Effect of Water Matrix and Pulsed Plasmas Waveform on Physicochemical Water Properties, Species Formation and Inactivation Efficiency of Escherichia Coli", *Environmental Research*, 266, 120467, 2024. <https://doi.org/10.1016/j.envres.2024.120467>
- [9] Carranzo, I. V. "APHA, AWWA, WEF. Standard Methods for examination of water and wastewater", *Anales de Hidrología Médica*, 5(2), pp. 185–186, 2012. [https://doi.org/10.5209/rev\\_anhm.2012.v5.n2.40440](https://doi.org/10.5209/rev_anhm.2012.v5.n2.40440)
- [10] BIS "IS 3025 (Part 34): Method of Sampling and Test (Physical and Chemical) for Water and Wastewater, Part 34: Nitrogen (First Revision)", Bureau of Indian Standards, New Delhi, India, 1988.

- [11] Standard Methods Committee of the American Public Health Association, American Water Works Association, and Water Environment Federation "4500-NO<sub>2</sub>- nitrogen (nitrite)", In: Lipps, W. C., Baxter, T. E., Braun-Howland, E. (eds.) Standard Methods For the Examination of Water and Wastewater, APHA Press, 2017. ISBN 978-0-87553-299-8  
<https://doi.org/10.2105/SMWW.2882.088>
- [12] Zhao Y. Y., Wang, T., Ren, Q. C., Wilson, M. P., Macgregor, S. J., Timoshkin, I. V. "Hydroxyl Radicals and Hydrogen Peroxide Formation at Nonthermal Plasma–Water Interface", *IEEE Transactions on Plasma Science*, 44(10), pp. 2084–2091, 2016.  
<https://doi.org/10.1109/tps.2016.2547841>
- [13] Piskarev, I. M. "The Formation of Ozone-Hydroxyl Mixture in Corona Discharge and Lifetime of Hydroxyl Radicals", *IEEE Transactions on Plasma Science*, 49(4), pp. 1363–1372, 2021.  
<https://doi.org/10.1109/tps.2021.3064785>
- [14] Boehm, D., Curtin, J., Cullen, P. J., Bourke, P. "Hydrogen Peroxide and Beyond-the Potential of High-voltage Plasma-activated Liquids Against Cancerous Cells", *Anti-Cancer Agents in Medicinal Chemistry*, 18(6), pp. 815–823, 2018.  
<https://doi.org/10.2174/1871520617666170801110517>
- [15] Hiroki, A., Laverne, J. A., Pimblott, S. M. "Hydrogen Peroxide Production in the Radiolysis of Water with High Radical Scavenger Concentrations", *The Journal of Physical Chemistry A*, 106(40), pp. 9352–9358, 2002.  
<https://doi.org/10.1021/jp0207578>
- [16] Bruggeman, P. J., Kushner, M. J., Locke, B. R., Gardeniers, J. G. E., Graham, W. G., Graves, Hofman-Caris, R. C. H. M., Maric, D., Reid, J. P., Ceriani, E. "Plasma–liquid interactions: a review and roadmap", *Plasma Sources Science and Technology*, 25(5), 053002, 2016.  
<https://doi.org/10.1088/0963-0252/25/5/053002>
- [17] Liu, D. X., Liu, Z. C., Chen, C., Yang, A. J., Li, D., Rong, M. Z., Chen, H. L., Kong, M. G. "Aqueous reactive species induced by a surface air discharge: Heterogeneous mass transfer and liquid chemistry pathways", *Scientific Reports*, 6(1), 23737, 2016.  
<https://doi.org/10.1038/srep23737>
- [18] Wu, M.-C., Uehara, S., Wu, J.-S., Xiao, Y.-C., Nakajima, T., Sato, T. "Dissolution enhancement of reactive chemical species by plasma-activated microbubbles jet in water", *Journal of Physics D: Applied Physics*, 53(48), 485201, 2020.  
<https://doi.org/10.1088/1361-6463/abae96>
- [19] Park, J. Y., Park, S., Choe, W., Yong, H. I., Jo, C., Kim, K. "Plasma-Functionalized Solution: A Potent Antimicrobial Agent for Biomedical Applications from Antibacterial Therapeutics to Biomaterial Surface Engineering", *ACS Applied Materials & Interfaces*, 9(50), pp. 43470–43477, 2017.  
<https://doi.org/10.1021/acsami.7b14276>
- [20] Galdeano, M. C., Wilhelm, A. E., Borges Goulart, I., Valeriano Tonon, R., Freitas-Silva, O., Germani, R., Hidalgo Chávez, D. W. "Effect of water temperature and pH on the concentration and time of ozone saturation", *Brazilian Journal of Food Technology*, 21, e2017156, 2018.  
<https://doi.org/10.1590/1981-6723.15617>
- [21] Cadorin, B. M., Tralli, V. D., Ceriani, E., de Brito Benetoli, L. O., Marotta, E., Ceretta, C., Debacher, N. A., Paradisi, C. "Treatment of methyl orange by nitrogen non-thermal plasma in a corona reactor: The role of reactive nitrogen species", *Journal of Hazardous Materials*, 300, pp. 754–764, 2015.  
<https://doi.org/10.1016/j.jhazmat.2015.08.009>
- [22] Bian, W., Song, X., Liu, D., Zhang, J., Chen, X. "Actions of nitrogen plasma in the 4-chlorophenol degradation by pulsed high-voltage discharge with bubbling gas", *Chemical Engineering Journal*, 219, pp. 385–394, 2013.  
<https://doi.org/10.1016/j.cej.2012.12.074>
- [23] Chen, J., Davidson, J. H. "Ozone Production in the Positive DC Corona Discharge: Model and Comparison to Experiments", *Plasma Chemistry and Plasma Processing*, 22(4), pp. 495–522, 2002.  
<https://doi.org/10.1023/a:1021315412208>
- [24] Chen, J., Wang, P. "Effect of relative humidity on electron distribution and ozone production by DC coronas in air", *IEEE Transactions on Plasma Science*, 33(2), pp. 808–812, 2005.  
<https://doi.org/10.1109/tps.2005.844530>
- [25] Weitzberg, E., Hezel, M., Lundberg, J. O., Warner, D. S. "Nitrate-Nitrite-Nitric Oxide Pathway", *Anesthesiology*, 113(6), pp. 1460–1475, 2010.  
<https://doi.org/10.1097/aln.0b013e3181fcf3cc>
- [26] Husain, D., L. J. Kirsch, L. J., Wiesenfeld, J. R. "Collisional quenching of electronically excited nitrogen atoms, N(2<sub>2</sub>D<sub>J</sub>, 2<sub>2</sub>P<sub>J</sub>) by time-resolved atomic absorption spectroscopy", *Faraday Discussions of the Chemical Society*, 53, pp. 201–210, 1972.  
<https://doi.org/10.1039/dc9725300201>
- [27] Lukes, P., Dolezalova, E., Sisrova, I., Clupek, M. "Aqueous-Phase Chemistry and Bactericidal Effects from an Air Discharge Plasma in Contact with Water: Evidence for the Formation of Peroxynitrite through a Pseudo-Second-Order Post-Discharge Reaction of H<sub>2</sub>O<sub>2</sub> and HNO<sub>2</sub>", *Plasma Sources Science and Technology*, 23(1), 015019, 2014.  
<https://doi.org/10.1088/0963-0252/23/1/015019>
- [28] Hoeben, W. F. L. M., Pemen, A. J. M., Huiskamp, T., Van Ooij, P. P., Lukeš, P., Schram, D. C. "On the Possibilities of Straightforward Characterization of Plasma Activated Water", *Plasma Chem Plasma Process*, 39(3), pp. 597–626, 2019.  
<https://doi.org/10.1007/s11090-019-09976-7>
- [29] Bolouki, N., Kuan, W.-H., Hsieh, J.-H., Huang, Y.-Y. "Characterizations of a Plasma-Water System Generated by Repetitive Microsecond Pulsed Discharge with Air, Nitrogen, Oxygen, and Argon Gases Species", *Applied Sciences*, 11(13), 6158, 2021.  
<https://doi.org/10.3390/app11136158>